PNAS RESEARCH ARTICLE | IMMUNOLOGY AND INFLAMMATION

Myeloid caspase-8 restricts RIPK3-dependent proinflammatory IL-1β production and CD4 T cell activation in autoimmune demyelination

Sunja Kim[a], Hsueh Chung Lu[a,b,1], Andrew J. Steelman[a,2], and Jianrong Li[a,b,3]

Edited by Hyun Kyoung Lee, Baylor College of Medicine, Houston, TX; received September 24, 2021; accepted May 5, 2022 by Editorial Board Member Hugo Bellen

Caspase-8 functions at the crossroad of programmed cell death and inflammation. Here, using genetic approaches and the experimental autoimmune encephalomyelitis model of inflammatory demyelination, we identified a negative regulatory pathway for caspase-8 in infiltrated macrophages whereby it functions to restrain interleukin (IL)-1β–driven autoimmune inflammation. Caspase-8 is partially activated in macrophages/microglia in active lesions of multiple sclerosis. Selective ablation of *Casp8* in myeloid cells, but not microglia, exacerbated autoimmune demyelination. Heightened IL-1β production by caspase-8–deficient macrophages underlies exacerbated activation of encephalitogenic T cells and production of GM-CSF and interferon-γ. Mechanistically, IL-1β overproduction by primed caspase-8–deficient macrophages was mediated by RIPK1/RIPK3 through the engagement of NLRP3 inflammasome and was independent of cell death. When instructed by autoreactive CD4 T cells in the presence of antigen, caspase-8–deficient macrophages, but not their wild-type counterparts, released significant amount of IL-1β that in turn acted through IL-1R to amplify T cell activation. Moreover, the worsened experimental autoimmune encephalomyelitis progression in myeloid *Casp8* mutant mice was completely reversed when *Ripk3* was simultaneously deleted. Together, these data reveal a functional link between T cell-driven autoimmunity and inflammatory IL-1β that is negatively regulated by caspase-8, and suggest that dysregulation of the pathway may contribute to inflammatory autoimmune diseases, such as multiple sclerosis.

multiple sclerosis | myeloid cells | inflammasome | caspase-8 | EAE

Significance

Autoimmune demyelination is driven by pathogenic T cells and inflammatory myeloid cells. How myeloid and T cells functionally interact and contribute to inflammatory demyelinating disease, such as multiple sclerosis, remains incompletely understood. This study identifies a caspase-8–mediated pathway in macrophages that suppresses inflammasome-dependent interleukin-1β production and autoimmunity during inflammatory demyelination. The study provides insights into the interplay between infiltrated myeloid cells and autoreactive T cells in multiple sclerosis that may also have implications for other autoimmune inflammatory diseases.

Multiple sclerosis (MS) is a chronic inflammatory demyelinating disease of the central nervous system (CNS) featuring multifocal demyelinating lesions that are often associated with immune cell infiltrates, microglial activation, and astrogliosis (1). In experimental autoimmune encephalomyelitis (EAE), a largely $CD4^+$ T cell–driven autoimmune demyelination model of MS, myeloid lineage cells, such as inflammatory monocytes and neutrophils, critically contribute to neuroinflammation and CNS pathology (2, 3). Activation of infiltrating monocytes and resident microglia is prominent in inflamed CNS foci in this model; and intercellular collaborations between myeloid cells and encephalitogenic T cells are essential in driving EAE progression. However, the molecular pathways that regulate local CNS infiltrate activation remain incompletely understood.

Caspase-8 has emerged as a critical regulator of programmed cell death and inflammation (4–6). In addition to its canonical function in initiating the extrinsic apoptotic pathway downstream of death receptor ligation, caspase-8 inhibits necroptosis (7, 8) and regulates innate immune signaling (9, 10), virtually through interacting with adaptor proteins, such as FADD, cellular FLICE-inhibitory protein (cFLIP), and inflammasome adaptor ASC in signaling complexes and through proteolytically processing downstream substrates. Caspase-8 activation is tightly regulated as it functions at the crossroad of cell death, survival, and inflammation, often in a context- and cell-type–dependent manner. Both proximity-triggered autoproteolytic activation of caspase-8 in specific signaling complexes and catalytic activity-independent scaffolding function of caspase-8 have been demonstrated under immune challenged contexts (11, 12). For example, the homodimer of fully processed/activated caspase-8 induces apoptosis, whereas the limited catalytic activity of caspase-8/cFLIP heterodimer restricts RIPK1/RIPK3-dependent necroptosis by cleaving RIPK3 and preventing necrosome formation (13, 14). Caspase-8 regulates NLRP3 inflammasome formation independent of its enzymatic activity in dendritic cells (9) and up-regulates inflammatory cytokine transcripts through a process that does not require caspase-8 self-processing (11, 15). Conditional loss of caspase-8 in dendritic cells and keratinocytes results in chronic

Author affiliations: [a]Department of Veterinary Integrative Biosciences, Texas A&M University, College Station, TX 77843; and [b]Texas A&M Institute for Neuroscience, Texas A&M University, College Station, TX 77843

Author contributions: S.K. and J.L. designed research; S.K., H.C.L., and A.J.S. performed research; S.K. and J.L. analyzed data; and S.K. and J.L. wrote the paper.

The authors declare no competing interest.

This article is a PNAS Direct Submission. H.K.L. is a guest editor invited by the Editorial Board.

[1]Present address: Autoimmune Disease Therapy, Sorrento Therapeutics, San Diego, CA 92121.

[2]Present address: Department of Animal Sciences, University of Illinois Urbana–Champaign, Champaign, IL 61801.

[3]To whom correspondence may be addressed. Email: jrli@cvm.tamu.edu.

This article contains supporting information online at http://www.pnas.org/lookup/suppl/doi:10.1073/pnas.2117636119/-/DCSupplemental.

Published June 7, 2022.

inflammation due to enhanced inflammasome activation (16, 17) and excessive constitutive activation of IRF3 antiviral pathways (18). Our previous work suggests that focal cellular caspase-8 activity is required to suppress RIPK3-mediated programmed necrosis in cultured microglia activated by Toll-like receptor (TLR) agonists (7). However, specific functions of microglial caspase-8 in vivo remain to be explored. *CASP8* loss-of-function variants due to missense mutations appear to correlate with increased risks for Alzheimer's disease (19). Lower levels of caspase-8 transcript were found in MS patients with detectable gadolinium-enhancing lesions on MRI, an early event in forming new MS lesions (20, 21). Interestingly, *CASP8* polymorphism has been implicated in genetic association studies with primary progressive MS (22), and is one of the strongly suggestive autosomal non-MHC loci that influences MS susceptibility (23). Although accumulating evidence suggests that caspase-8 may function as a molecular rheostat for modulating cell death and inflammation, whether and how caspase-8 dysfunction or dysregulation contributes to inflammatory demyelination remains unclear.

Myeloid cells including microglia are innate immune cells that express high levels of caspase-8 in mice and humans (24–26). In this study, we demonstrate increased levels of partially processed caspase-8 in activated microglia/macrophages at the border of actively demyelinating lesions in postmortem MS tissues. Activated caspase-8 in association with NLRP3$^+$ aggregates were found in infiltrating monocyte-derived macrophages at demyelinating foci during the early phase of EAE. Conditional deletion of *Casp8* in myeloid cells exacerbated neuroinflammation and clinical EAE symptoms, whereas selective ablation of *Casp8* in the CNS microglial cells did not impact disease development and progression, suggesting that activated caspase-8 in infiltrating myeloid cells restricts autoimmune inflammation. We further identified that increased interleukin (IL)-1β secretion through RIPK3-dependent inflammasome activation in the absence of myeloid caspase-8 underlies heightened encephalitogenic CD4$^+$ T cell immune activation. This study demonstrates an in vivo role for myeloid caspase-8 in restricting inflammasome-meditated IL-1β overproduction, thereby functioning as a negative checkpoint against excessive pathogenic effector T cell activity during autoimmune encephalomyelitis.

Results

Caspase-8 Is Cleaved/Activated in Microglia/Macrophages in Actively Demyelinating Lesions of MS. Peripheral myeloid cells and CNS microglia substantially contribute to the neuroinflammatory process, demyelination, and axonal damage in MS and EAE (3, 27). Transcriptomic analysis shows abundant *Casp8* and *Cflar*, which encodes cFLIP, expression in both human and mouse CNS microglia/macrophages (*SI Appendix*, Fig. S1 *A–C*), suggesting a potential role in regulating microglia/macrophage function. Using BAC transgenic *Casp8-egfp* reporter mice, where EGFP is expressed under the regulation of the *Casp8* promoter to visualize caspase-8 expression, we confirmed that caspase-8 is predominantly expressed in Iba1$^+$ microglia and perivascular macrophages in normal adult brain and spinal cord (*SI Appendix*, Fig. S1*D*), as well as in significant populations of splenic and circulating monocytes, neutrophils, and lymphocytes (*SI Appendix*, Fig. S1 *E* and *F*).

Procaspase-8 undergoes various proteolytic cleavage at several specific sites for conformational and enzymatic activation. Using an antibody that explicitly detects several cleaved/activated forms of caspase-8, we examined postmortem MS tissues and observed abundant expression of processed caspase-8 near the lesion, especially on the expanding edge where active demyelination is apparent (Fig. 1 *A* and *B*). Interestingly, cleaved caspase-8 was localized to tomato lectin-positive microglia/macrophages that exhibited diverse morphology, ranging from hypertrophic cell bodies with a few processes at the lesion border to ameboid phagocytes with engulfed myelin debris in the demyelinated lesion (Fig. 1 *C* and *D*). Confocal microscopy revealed discrete caspase-8$^+$ puncta in microglia/macrophages, suggesting processed caspase-8 in intracellular compartments or aggregation of protein complexes (Fig. 1*E*). Of note, these caspase-8$^+$ microglia/macrophages did not appear to be degenerating. Western blot analysis revealed significant increases of partially processed caspase-8 (p43/45) in MS brains when compared to controls (Fig. 1*F*), whereas the level of the p18 fragment of fully processed caspase-8 was not statistically different (Fig. 1*G*). Activated microglia/macrophages in and around actively demyelinating MS lesions express the antigen presentation molecule major histocompatibility complex class II (MHCII) (27). As caspase-8 has been previously shown to negatively regulate MHCII in bone marrow-derived dendritic cells (28), we examined caspase-8 and MHCII expression in MS tissues. Integrative intensity analysis showed that while both cleaved caspase-8 and MHCII are abundantly expressed in the active lesion border area, the intensity of caspase-8 was inversely correlated with MHCII (*SI Appendix*, Fig. S2). Together, these results showed that caspase-8 is significantly activated and clustered in subsets of macrophages/microglia in actively demyelinating MS lesions as compared to normal-appearing white matter or control brains. The distinct spatial accumulation of partially processed caspase-8 in macrophages/microglia raises the question whether myeloid caspase-8 activation regulates CNS inflammation and demyelination.

Myeloid Cell-Specific Ablation of *Casp8* Results in Exacerbated EAE Progression. To study the role of myeloid caspase-8 in the pathogenesis of autoimmune demyelination, we first examined whether caspase-8 is activated in the $MOG_{35–55}$–induced EAE model of MS using a myeloid cell reporter line. The transgenic mice (*LysM^{cre}:Ai14*) harbor a floxed Stop-Td-tomato allele in the Rosa26 locus that, upon *lysozyme M* (*LysM*) promoter-mediated recombination, selectively labels peripheral myeloid cells, such as macrophages, monocytes, and neutrophils, and to a much less extent the CNS microglia (29). At the peak of EAE, Td-tomato$^+$ myeloid cells populated the inflamed spinal foci (Fig. 2*A*). Interestingly, robust proteolytic activation of caspase-8 was observed in Td-tomato$^+$ myeloid cells in the lesion area (Fig. 2*A*). Moreover, *Casp8* transcript was significantly increased in the spinal cord of EAE mice (Fig. 2*B*). These data suggest that caspase-8 is up-regulated transcriptionally and activated in myeloid cells during inflammatory demyelination.

To determine the functional role of *Casp8* in EAE pathogenesis, we used the Cre/LoxP system to generate two separate lines of conditional knockout mice: one with *Casp8* inducibly ablated in microglia using the *Cx3cr1* promoter, and one with *Casp8* specifically deleted in myeloid cells using the *LysM* promotor. Using *Cx3cr1$^{creERt/+}$:Ai14* and *LysM^{cre}:Ai14* reporter mice, we have recently confirmed that *LysM$^{cre/+}$* induces efficient gene recombination in peripheral myeloid lineage cells, including monocytes and granulocytes, whereas selective microglial gene targeting is achieved in inducible *Cx3cr1$^{creERt/+}$* mice 4 wk after tamoxifen treatment (29).

Both *Cx3cr1$^{creERt/+}$ Casp8$^{fl/fl}$* (*C8KO^{Cx3cr1}*) and *LysM$^{cre/+}$ Casp8$^{fl/fl}$* (*C8KO^{LysM}*) mice were born with normal Mendelian segregation and appeared to develop normally. Constitutive *C8KO^{LysM}* mutant mice were indistinguishable from their littermate wild-type (WT) controls and exhibited comparable myelination as WT (*SI*

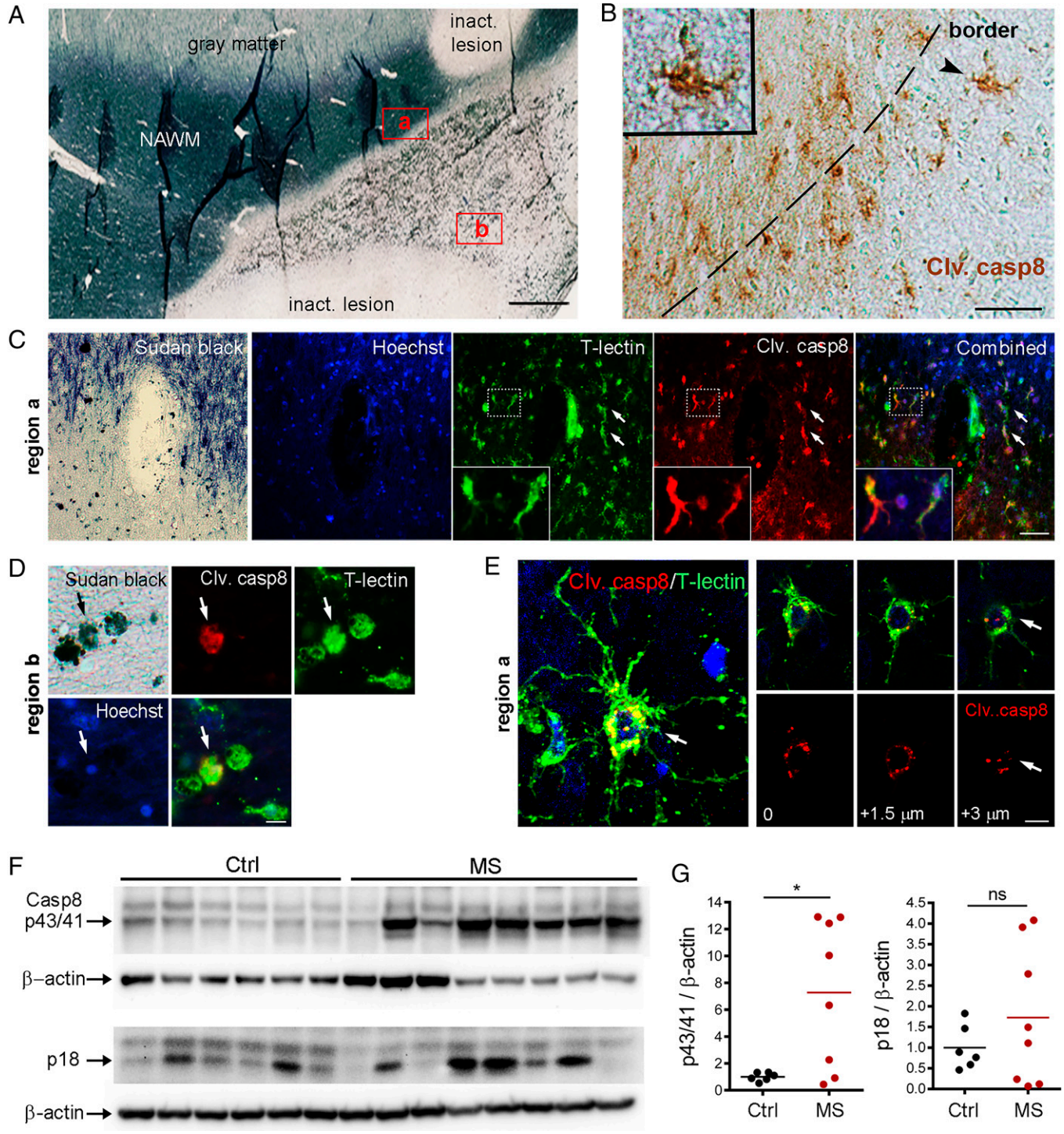

Fig. 1. Caspase-8 is proteolytically activated in microglia/macrophages in demyelinating MS lesions. (*A*) Representative photomicrograph of postmortem MS brain tissues stained with neutral lipid dye Sudan black showing actively demyelinating lesion area with myelin debris (region b) and the borderline (region a). Inact. lesion, chronic inactive demyelinated lesion; NAWM, normal-appearing white matter. (Scale bar, 1 mm.) (*B*) Representative immunofluorescence images for cleaved/activated caspase-8 (clv. casp8) near the lesion border. Positive cells exhibited morphology characteristic of microglia/macrophages. (*Inset*) 1.7× magnified view of a cleaved casp8^{+} cell (arrowhead). (Scale bar, 50 µm.) (*C*) Double immunofluorescence staining showing most active caspase-8^{+} cells were Td-tomato^{+} microglia/macrophages (arrows). (*Inset*) Representative double-positive cells at 3.3× higher magnification. (Scale bar, 50 µm.) (*D*) Representative photomicrograph of a cleaved caspase-8^{+} macrophage containing engulfed myelin debris in the active lesion. (Scale bar, 10 µm.) (*E*) Three-dimensional compiled confocal images (*z*-stack depth 8 µm) of a representative microglia/macrophage containing local cleaved caspase-8 in the lesion border region (a). Intracellular caspase-8 signals at three single *z*-stack confocal planes were shown on the right. (Scale bar, 10 µm.) (*F* and *G*) Western blot analysis of proteolytically cleaved caspase-8 fragments, a partially processed p43, and fully processed subunit p18, in postmortem brain tissues from patients with MS and controls. Densitometry analysis shows significant elevation of caspase-8 p43 fragment in MS tissues as compared to controls. Data represent the mean of each sample. Control cases, $n = 6$; MS cases, $n = 8$. *$P < 0.05$; ns, not significant.

Appendix, Fig. S3). Tamoxifen treatment of adult *C8KO*^{Cx3cr1} mice results in efficient genomic deletion of *Casp8* in microglia (*SI Appendix*, Fig. S4). However, loss of microglial *Casp8* did not affect EAE development nor its progression (Fig. 2 *C* and *D*). In contrast, *C8KO*^{LysM} mutant mice exhibited accelerated EAE progression with a significantly earlier disease onset (Fig. 2 *E*–*G*).

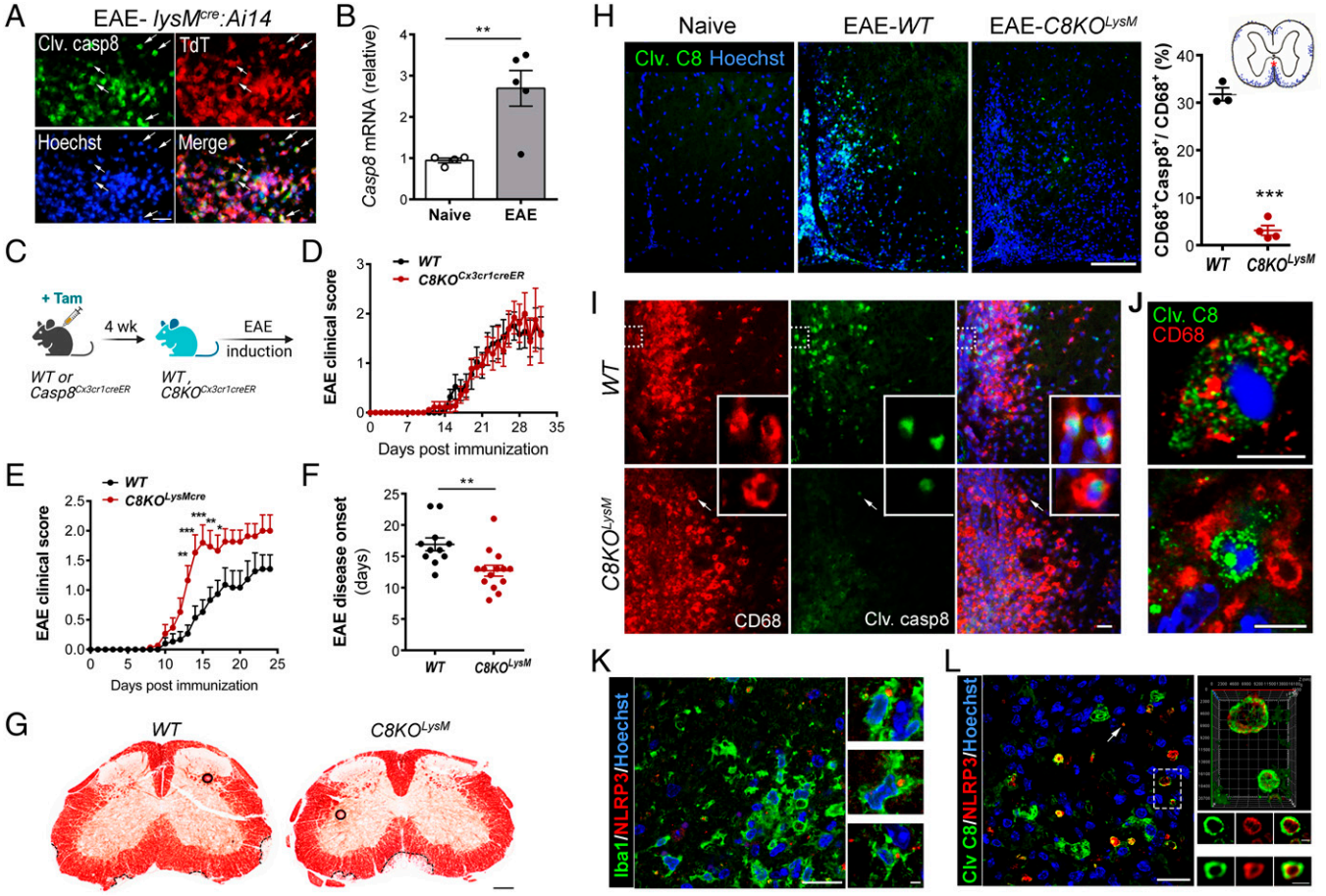

Fig. 2. Ablation of *Casp8* in peripheral myeloid cells but not in microglia exacerbates disease onset and CNS inflammation in EAE. (*A* and *B*) Caspase-8 is up-regulated and activated in infiltrating myeloid cells in the inflamed foci during EAE. Myeloid cell reporter mice (*LysM* ^{cre}*:Ai14*) were subject to $MOG_{35–55}$–induced EAE, and at the peak of disease (2 wk postimmunization, average clinical scores = 2), the spinal cords were immunostained for cleaved/active caspase-8 (*A*) or subjected to quantitative RT-PCR analysis (*B*). Arrows, colocalization of cleaved caspase-8 immunoreactive signal to Td-tomato$^+$ myeloid cells. Naïve mice, $n = 4$; EAE, $n = 5$. $^{**}P < 0.01$; Student t test. (Scale bar, 20 μm.) (*C* and *D*) Overall experimental scheme for tamoxifen-induced *Casp8* ablation in microglia. EAE was induced 4 to 5 wk after tamoxifen treatment. Mean EAE clinical scores and progression were indistinguishable between microglial *Casp8* knockout (*C8KO*^{Cx3cr1}) and littermate control mice (WT). Data represent mean ± SEM of five independent experiments. WT, $n = 22$; *C8KO*^{Cx3cr1}, $n = 18$. (*E* and *F*) Mean EAE clinical scores and disease onset of immunized myeloid-specific *Casp8* knockout mice (*C8KO*^{LysM}) and littermate controls (WT). Data represent mean ± SEM of three independent experiments. $n = 15$ per genotype. $^{*}P < 0.05$; $^{**}P < 0.01$; $^{***}P < 0.001$; two-way ANOVA with Bonferroni's multiple comparison tests (*E*). $^{**}P < 0.01$; Student t test (*F*). (*G*) Representative photomicrographs of lumbar spinal cord sections stained with Oil red O for myelin. Dashed lines denote demyelinated areas. (Scale bar, 200 μm.) (*H*) Representative cleaved caspase-8 immunostaining of lumbar spinal cord sections from naïve mice and EAE WT and *C8KO*^{LysM} mice at 2-wk postimmunization. The *Right* panel is a transverse schematic of lumbar spinal sections of EAE mice showing CD68$^+$ macrophage-populated areas. The red asterisk indicates the area quantitatively analyzed for cleaved caspase-8$^+$ CD68$^+$ cells. WT, $n = 3$; *C8KO*^{LysM}, $n = 4$. $^{***}P < 0.001$. (Scale bar, 100 μm.) (*I*) Representative EAE spinal sections immunostained for cleaved caspase-8 and CD68 at higher magnifications. The *Inset* in the lower *C8KO*^{LysM} panel indicates a cleaved caspase-8$^+$ cell phagocytosed by an CD68$^+$ cell. (Scale bars, 20 μm.) (*J*) Representative confocal images of EAE WT tissue showing punctuated/localized cleaved caspase-8 signal either spanning cytoplasm (*Upper*) or localized to the perinuclear area (*Lower*) in CD68$^+$ microglia/macrophages. (Scale bars, 5 μm.) (*K*) Abundant NLRP3 expression in Iba1$^+$ cells in the spinal cord lesion of WT mice 2 wk after EAE induction. Three representative Iba1$^+$ cells containing a NLRP3$^+$ speck are shown (*Right*) at a higher magnification. (Scale bars, 20 μm.) (*L*) Representative confocal images of EAE spinal tissue sections stained for NLRP3 and cleaved caspase-8. (*Inset Upper*) Three-dimensional maximum projection of confocal *z*-stack images showing NLRP3$^+$ specks (red) in association with cleaved caspase-8 (green). (*Lower*) Representative single-plane two-dimensional images of NLRP3$^+$/cleaved caspase-8$^+$ "rings". (Scale bars, 20 μm; 2 μm for *Insets*.)

Together, these results suggest that caspase-8 activation in infiltrated myeloid cells modulates the pathogenesis of EAE.

Immunohistochemical analyses with antibodies specific for cleaved caspase-8 showed that caspase-8 was not activated in naïve spinal cords, but it became robustly activated in CD68$^+$ macrophages in the inflammatory foci of the spinal cords of WT EAE mice (Fig. 2 *H* and *I*). This caspase-8 immunoreactivity was, however, largely abolished in myeloid *C8KO*^{LysM} EAE tissues, demonstrating the efficacy of caspase-8 inactivation and the specificity of the antibody. Approximately 30% of CD68$^+$ cells were positive for cleaved caspase-8, whereas less than 5% of CD68$^+$ cells were positive for cleaved caspase-8 in the *C8KO*^{LysM} EAE mice (Fig. 2*H*). These results suggest that peripheral myeloid cells account for most of the cleaved caspase-8 and CD68 double-positive cells in EAE and that loss of *Casp8* in infiltrating myeloid cells resulted in accelerated disease progression. Consistent with MS tissue findings, discrete expression patterns of cleaved caspase-8 were also detected in CD68$^+$ macrophages (Figs. 1*E* and 2*J*). In addition, we observed robust NLRP3 immunoreactivity in Iba1$^+$ cells in demyelinating lesions (Fig. 2*K* and *SI Appendix*, Fig. S5 *A* and *B*). Interestingly, although in general large aggregated immunoreactivity of cleaved caspase-8 did not colocalize with NLRP3, smaller speck-like and spheroid-shaped NLRP3$^+$ signals, in sizes of ∼2 to 8 μm, were directly associated with cleaved caspase-8 (Fig. 2*L*). Moreover, significantly more Iba1$^+$ cells in the *C8KO*^{LysM} EAE mice contained NLRP3$^+$ specks than the WT group (*SI Appendix*, Fig. S5*C*). Collectively, these data suggest that localized caspase-8 activation may negatively regulate the NLRP3

inflammasome, and that loss of caspase-8 releases the constraint resulting in increased NLRP3 inflammasome activation and neuroinflammation.

Activation of the NLRP3 inflammasome has been shown to contribute to EAE development and inflammatory leukocyte infiltration (30, 31). Depending on experimental induction protocols, EAE progresses via both NLRP3 inflammasome-dependent and NLRP3-independent pathogenic pathways. Induction with higher doses of MOG peptide or inactivated *Mycobacteria tuberculosis* resulted in an inflammasome-independent, Th17-dominated disease progression that was similar between WT and *Nlrp3*-, *Asc*-, or *Casp1*-deficient mice (32). In contrast, when lower doses of *M. tuberculosis* or MOG peptide was used, global *Nlrp3*, *Asc*, or *Casp1* deficiency suppressed EAE pathogenesis (32). When we used a higher dose of *M. tuberculosis* for EAE induction, $C8KO^{LysM}$ mice still displayed a moderately earlier disease onset (*SI Appendix*, Fig. S6), although the difference between the genotypes was less evident than those if a lower amount of *M. tuberculosis* was used (Fig. 2). Therefore, the mild EAE induction regime was used for the rest of this study.

Myeloid-Specific *Casp8* Deficiency Enhances Th1 Responses in the CNS of EAE Mice. To understand the basis underlying the enhanced pathogenesis in $C8KO^{LysM}$ mice, we examined mononuclear cells from the CNS at the peak of the disease. While the number and percentage of $CD11b^+$ $CD45^{int}$ microglia remained the same between genotypes, a significant increase of infiltrated monocytes/macrophages ($CD11b^+$ $CD45^{high}$) was found in the CNS of $C8KO^{LysM}$ mice (Fig. 3*A*). Lysozyme M-driven *cre* recombination is also efficient in granulocytes and myeloid dendritic cells (29); however, granulocyte ($Ly6G^+CD11b^+$) and dendritic cell ($CD11c^+CD11b^+$) populations were not different between genotypes (Fig. 3*A* and *SI Appendix*, Fig. S7). Nor were there differences in $CD8^+$ T cell and $B220^+$ B cell populations (*SI Appendix*, Fig. S7). In stark contrast, $CD11b^+MHCII^+$ cells were significantly increased in $C8KO^{LysM}$ mice as compared to WT as determined by flow cytometry as well as by immunohistochemistry analyses (Fig. 3 *B* and *C*). Consistent with elevated $CD11b^+MHCII^+$ cell population, there were significantly more $CD4^+$ T lymphocytes in the CNS of $C8KO^{LysM}$ mice than WT at the peak of disease (Fig. 3 *D* and *E*).

We next tested whether myeloid *Casp8* ablation results in enhanced antigen-specific immune responses in secondary lymphoid organs. Splenocytes from WT and $C8KO^{LysM}$ mice at the preclinical and disease onset time points responded to $MOG_{35–55}$ restimulation and produced similar levels of interferon (IFN)-γ and IL-17A, and $CD11b^+$ cells had similar level of surface MHCII (*SI Appendix*, Fig. S8 *A–D*). Moreover, mononuclear cells isolated from draining lymph nodes of WT and $C8KO^{LysM}$ mice during the preclinical phase also elicited similar antigen-specific immune responses between the genotypes (*SI Appendix*, Fig. S8*E*). In contrast to the periphery, CNS mononuclear cells from preclinical $C8KO^{LysM}$ mice exhibited stronger immune responses than WT upon antigen reactivation (Fig. 3*F*), and produced significantly more CCL2, consistent with aforementioned findings of increased $CD11b^+CD45^{hi}$ macrophages in $C8KO^{LysM}$ CNS at the peak of disease, as CCL2 is a key central signal for inflammatory monocyte infiltration during EAE. Importantly, IL-1β and IFN-γ were also significantly higher in CNS mononuclear cells from $C8KO^{LysM}$ mice than those from the WT (Fig. 3*F*), suggesting that local IL-1β production and enhanced Th1 effector responses in the CNS of $C8KO^{LysM}$ mice underlies the exacerbated EAE progression when myeloid *Casp8* is ablated.

Caspase-8 Deficiency Results in Spontaneous Caspase-1–Dependent Production of IL-1β in Lipopolysaccharide-Activated Bone Marrow-Derived Macrophages. To investigate the molecular mechanism governing the effect of *Casp8* ablation, we next used in vitro approaches and analyzed immune responses of bone marrow-derived macrophages (BMDM) from WT and $C8KO^{LysM}$ mice upon activation. We confirmed that BMDM from $C8KO^{LysM}$ mice had attenuated caspase-8 expression as compared to WT BMDM (*SI Appendix*, Fig. S9). Lipopolysaccharide (LPS) treatment transcriptionally up-regulated immune molecules, such as *Tnf*, *Il1b*, *Il6*, *Il12*, and *Ccl2* in WT and $C8KO^{LysM}$ BMDM to a similar extent (Fig. 4*A*). However, *Casp8*-deficient macrophages produced significantly higher levels of mature IL-1β, while tumor necrosis factor (TNF), IL-6, IL-12, and CCL2 production was not different between LPS-stimulated WT and *Casp8*-deficient BMDM (Fig. 4*B*). Notably, we did not detect differences in cell death under both basal and LPS-stimulated conditions (*SI Appendix*, Fig. S10), suggesting that *Casp8*-deficient macrophages possess enhanced capacity in producing mature IL-1β independent of cell death.

Our in vivo results suggest that NLRP3 is expressed and colocalized with cleaved caspase-8 in speck-like structures in myeloid cells around inflammatory lesions (Fig. 2). Caspase-8 has been shown previously to be necessary for canonical and noncanonical NLRP3 inflammasome activation and IL-1β production (33, 34), and is also capable of directly processing pro–IL-1β independent of inflammasome (35). However, an opposing inhibitory function of caspase-8 in IL-1β production was also reported in LPS-activated dendritic cells (16). Because of the highly inflammatory nature of IL-1β, its production is tightly regulated and generally requires two signaling steps (34, 36). The first step, termed priming, involves transcriptional up-regulation of *Il1b* and some inflammasome components through NF-κB activation, usually after TLR activation. The second is inflammasome assembly/activation and pro–IL-1β processing into mature IL-1β, which can be trigged by a variety of stimuli, including danger signals such as ATP, uric acid, and particulate matters.

We found that *Casp8* ablation had no effect on LPS-induced transcriptional up-regulation of *Il1b* (Fig. 4*A*) but resulted in spontaneous release of mature IL-1β in the absence of additional inflammasome stimulator (Fig. 4*B*). This spontaneous IL-1β production by LPS-activated *Casp8*–deficient macrophages was dependent on caspase-1 activation, as caspase-1 inhibitor YVAD-fmk effectively abolished IL-1β production (Fig. 4*C*). As expected, LPS alone did not induce IL-1β maturation in WT macrophages but addition of nigericin, a classic NLRP3 inflammasome activator, triggered robust IL-1β secretion (Fig. 4*C*). Nigericin further increased IL-1β production in LPS-stimulated *Casp8*-deficient macrophages to an extent comparable to that of WT cells (Fig. 4*C*), suggesting that in macrophages activated by low doses of LPS caspase-8 constitutively represses NLRP3/caspase-1 activation. As reactive oxygen species (ROS) may activate NLRP3 inflammasome independent of cell death (37), we asked whether *Casp8*-deficient macrophages produce more ROS than their WT counterparts. Indeed, we found significantly greater levels of ROS in *Casp8*-deficient macrophages upon LPS stimulation, which was completely abolished by the antioxidant butylated hydroxyanisole (BHA) (Fig. 4*D*). Similarly, BHA abrogated IL-1β production in LPS-treated *Casp8*-deficient macrophages (Fig. 4*E*). Taken together,

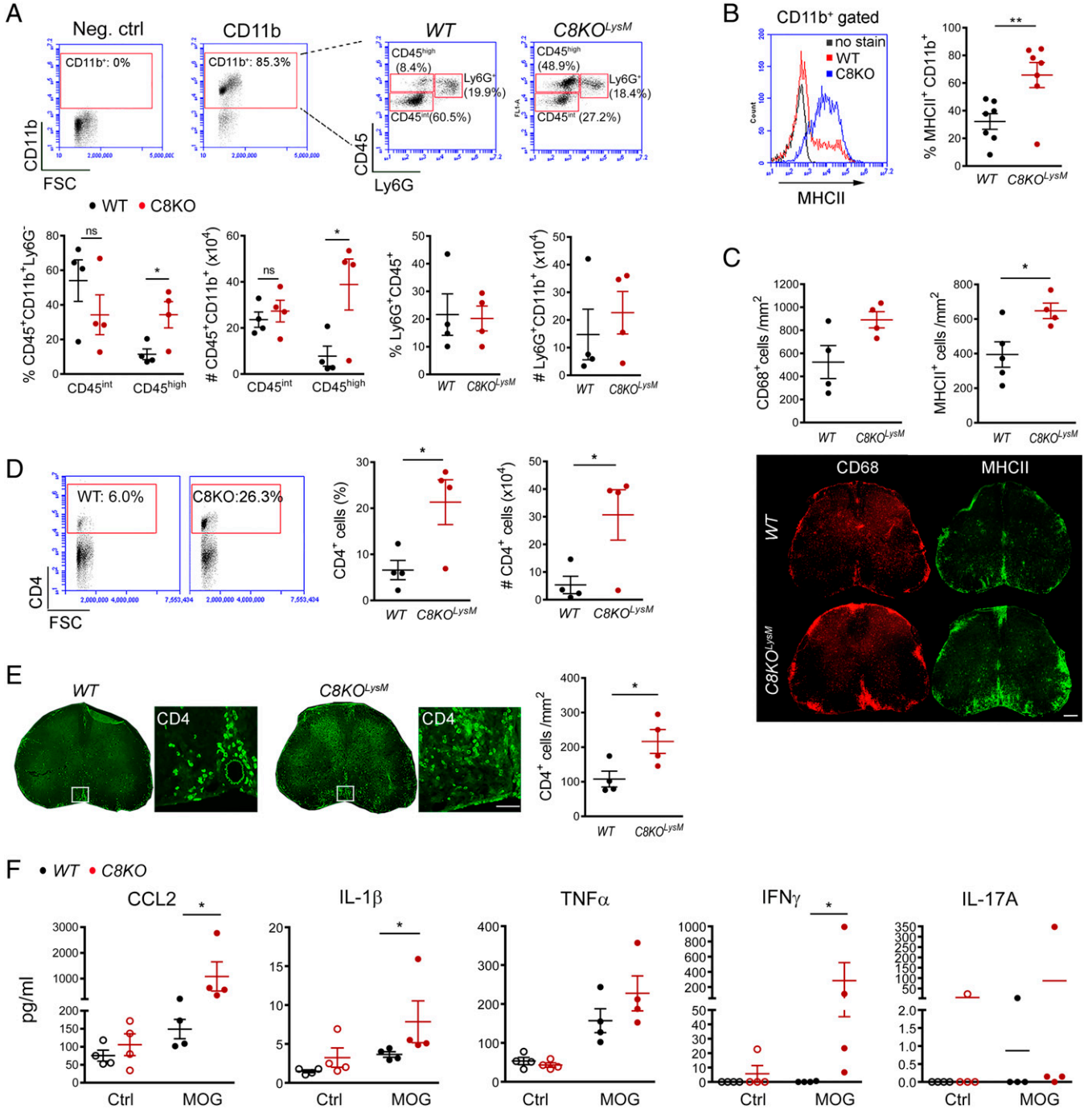

Fig. 3. Myeloid-specific loss of *Casp8* augments Th1 responses in the CNS of EAE mice. (*A*) Flow cytometry analysis of myeloid cells in the CNS of EAE mice. Mononuclear cells were isolated from spinal cords of WT and *C8KO^{LysM}* mice 2 wk after $MOG_{35–55}$ immunization. The population of infiltrated macrophages ($CD11b^+$ $CD45^{high}$) was significantly greater in *C8KO^{LysM}* than WT mice. Microglia ($CD11b^+$ $CD45^{int}$), neutrophil ($CD11b^+Ly6G^+$), and dendritic cell ($CD11c^+CD11b^+$) populations were not significantly different between genotypes. Data are presented as the percentage of $CD11b^+$ cells as well as total cell numbers of specified cell populations. $n = 3$ to 4 mice per genotype. (*B*) Flow cytometry analysis of MHCII surface expression levels and $MHCII^+$ myeloid cell populations in WT and *C8KO^{LysM}* mice. $n = 7$ mice per genotype. (*C*) Immunohistochemistry analysis of macrophages/microglia in the lumbar spinal cord of WT and *C8KO^{LysM}* EAE mice. (*Upper*) Quantitative $CD68^+$ and $MHCII^+$ cell analysis. (*Lower*) Representative images of lumbar spinal cord sections stained with anti-CD68 and MHCII antibodies. $n = 4$ mice per genotype. (Scale bar, 200 μm.) (*D* and *E*) Flow cytometry and immunohistochemistry analysis of $CD4^+$ T helper cells showing increased $CD4^+$ T cell infiltration into the CNS of *C8KO^{LysM}* mice as compared to WT. Boxes denote the lesion area shown at a higher magnification and quantified. $n = 4$ mice per genotype. (Scale bar, 50 μm.) (*F*) Antigen-specific responses of mononuclear cells isolated from spinal cords of WT and *C8KO^{LysM}* mice at preclinical stage of EAE (10 d postinfection). The CNS mononuclear cells were restimulated with or without $MOG_{35–55}$ (30 μg/mL) for 72 h, and the levels of cytokines/chemokines in the supernatant were analyzed by multiplex immunoassay. $n = 4$ mice per genotype. Data are a representative of three independent experiments. For IL-1β and IFN-γ, the difference between genotypes was analyzed using nonparametric Mann–Whitney *U* test. Data present mean ± SEM, $*P < 0.05$; $**P < 0.0.1$; ns, not significant.

these data suggest that caspase-8 deficiency in macrophages results in increased ROS production upon LPS stimulation, which leads to conventional NLRP3 activation and caspase-1–mediated IL-1β maturation.

Increased Macrophage IL-1β Production Promotes Antigen-Specific T Helper Cell Activation. To determine the potential role of enhanced IL-1β production from *C8KO^{LysM}* macrophages in reciprocal interactions with encephalitogenic T cells in pathological

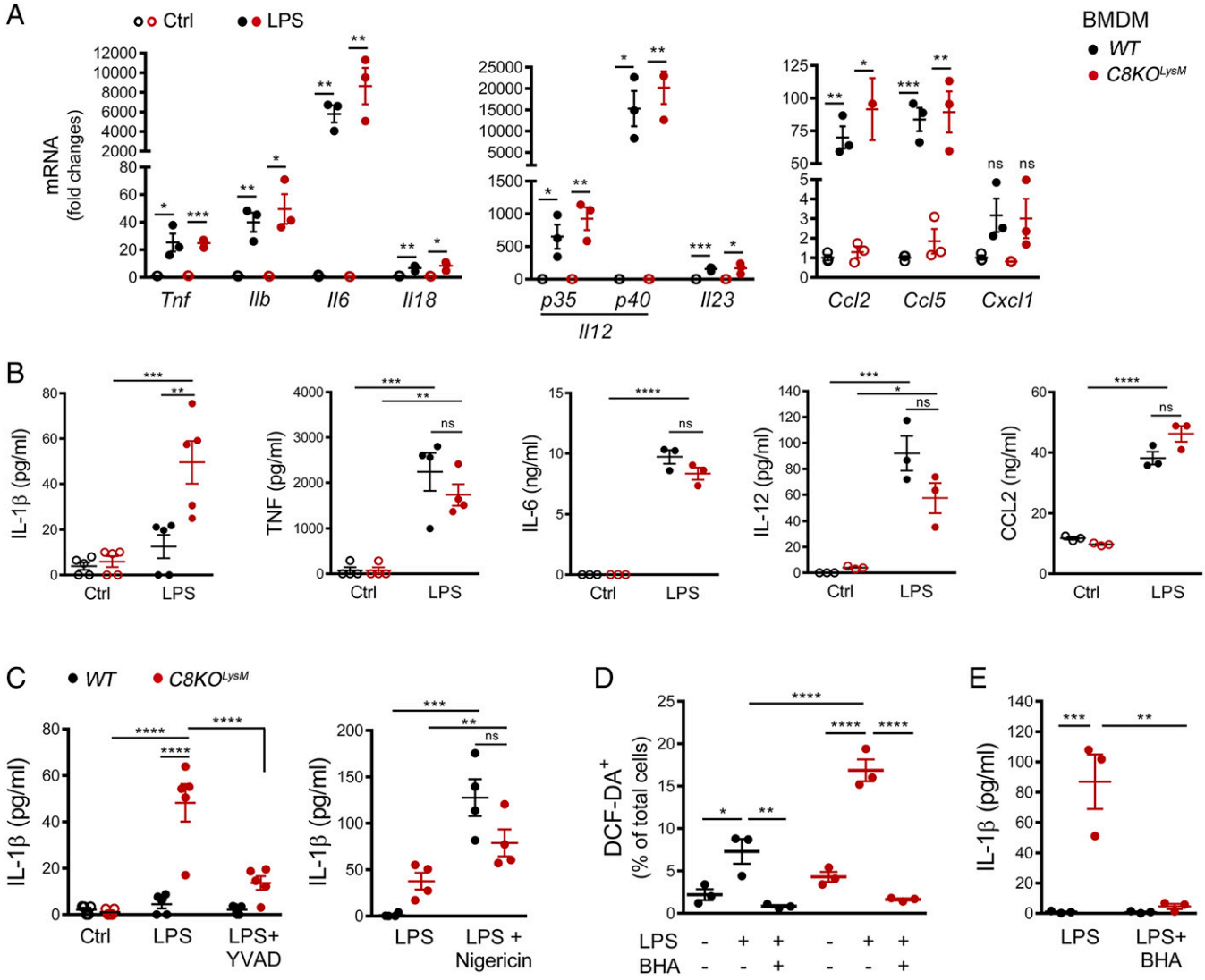

Fig. 4. *Casp8*-deficient BMDM produce more IL-1β through intrinsic activation of inflammasome. (*A*) Quantitative RT-PCR analysis of transcriptional up-regulation of cytokines and chemokines in BMDM 5 h after LPS (10 ng/mL) stimulation. Data dots represent biological replicates (n = 3 mice per genotype). (*B*) Cytokine/chemokine protein levels in culture supernatants from WT and *C8KO*^{LysM} BMDM treated with LPS for 24 h. n = 3 to 5 biological replicates per genotype. (*C*) Effect of caspase-1 inhibitor and nigericin on IL-1β production by LPS-activated WT and *C8KO*^{LysM} macrophages. BMDM were treated with LPS (10 ng/mL), caspase-1 inhibitor YVAD (20 μM), and nigericin (10 μg/mL) as indicated for 6 h and IL-1β in the culture supernatants was measured by ELISA. n = 4 to 5 per genotype. (*D*) Heightened ROS production by *C8KO*^{LysM} BMDM upon LPS activation and complete inhibition by antioxidant BHA. ROS production was evaluated with DCF-DA at 4 h after LPS treatment. Cotreatment with BHA (200 μM) abolished LPS-induced ROS production. n = 3 per genotype. (*E*) BHA completely prevented IL-1β production when measured at 24 h after LPS stimulation. n = 3 per genotype; *P < 0.05, **P < 0.0.1, ***P < 0.001.

processes, we cocultured MOG-reactive CD4$^+$ T cells with *Casp8* WT or deficient microglia and BMDM in the presence of cognate antigen MOG$_{35–55}$ peptide (Fig. 5*A*). Mixed glia cultures were used to evaluate the capacity of microglial caspase-8 on T cell immune responses. We first confirmed that hydroxy-tamoxifen induced cre recombinaiton specifically in microglia as determined by reporter expression (*SI Appendix*, Fig. S11 *A* and *B*) and that microglial *Casp8* ablation resulted in moderate increases in LPS-elicited IL-1β production when compared to WT microglia (*SI Appendix*, Fig. S11*C*). In the presence of exogenously added MOG peptide, autoreactive T cells cocultured with mixed glia increased IFN-γ production; however, no genotype differences were observed (Fig. 5*B*). Moreover, no IL-1β secretion was detected in the mixed glia and T cell cocultures. In stark contrast, CD4$^+$ T cells cocultured with caspase-8–deficient BMDM were robustly activated in the presence of MOG antigen, producing more IFN-γ than those cocultured with WT BMDM (Fig. 5*B*). In addition to enhanced antigen-specific IFN-γ production, other pathogenic cytokines produced by Th cells—such as GM-CSF, IL-17A, and IL-23—were all markedly increased upon the loss of myeloid *Casp8* (Fig. 5*C*). These results show that caspase-8–deficient macrophages promote Th cell activation and effector responses, which is consistent with our in vivo finding of exacerbated EAE in *C8KO*^{LysM} but not microglia *C8KO*^{Cx3cr1} mice when compared to WT mice (Fig. 2*D*).

To rule out the possibility that *Casp8* ablation affected macrophage or T cell survival, CD3$^+$ T cells and Iba1$^+$ macrophages were counted at 48 h after antigen stimulation. The number of T cells under the control condition was similar between the genotypes, and was moderately increased in *C8KO*^{LysM} cocultures under MOG-stimulated conditions, yet remained comparable to that of the WT cocultures (*SI Appendix*, Fig. S12*A*). This implies that increased IFN-γ production in MOG-treated *C8KO* cocultures (Fig. 5*B*) was not simply due to changes in T cell numbers. Moreover, the

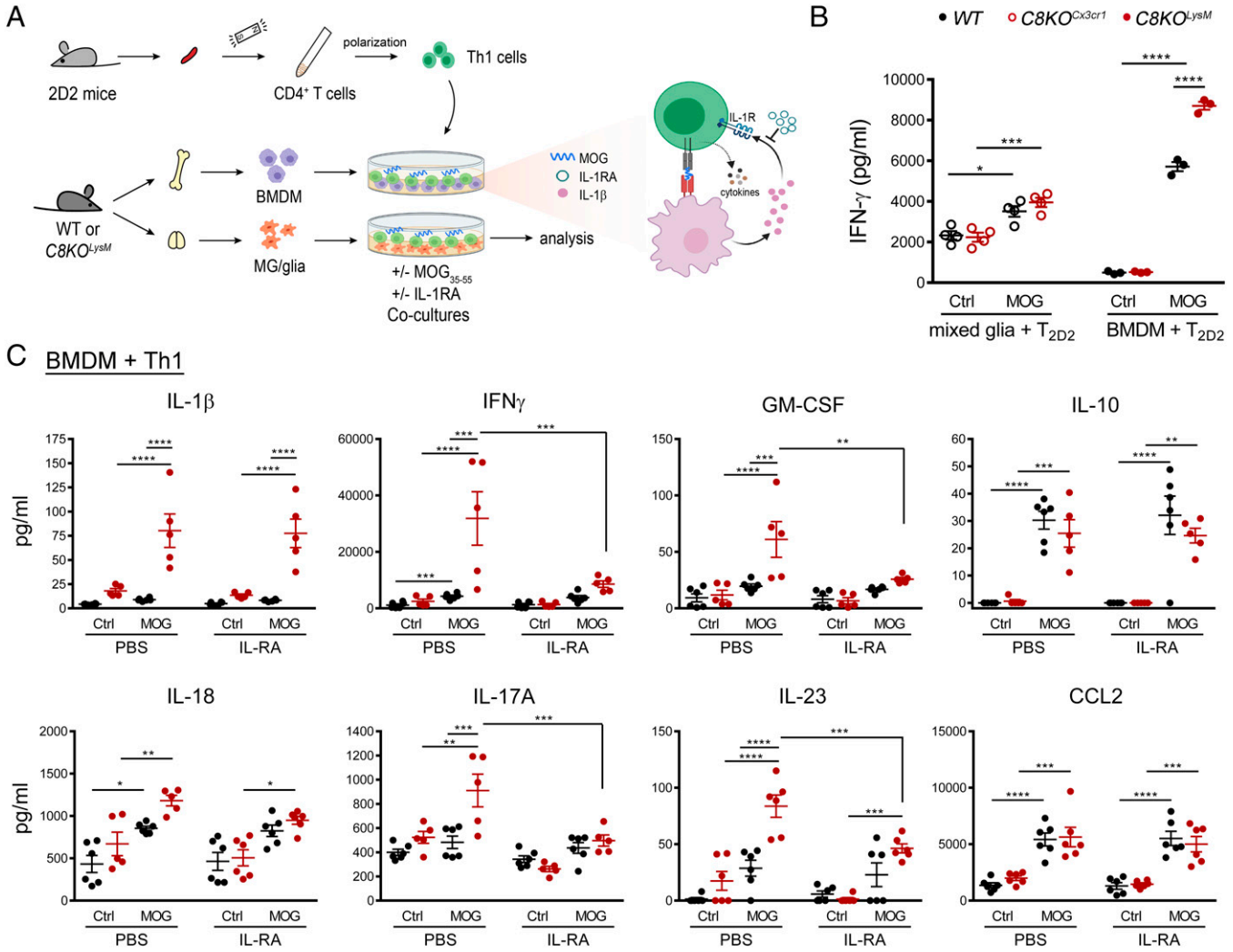

Fig. 5. Increased IL-1β production from caspase-8–deficient BMDM is responsible for enhanced T cell activation. (*A*) Schematic diagram of the experimental design. BMDM or mixed glia were cocultured with Th1 polarized 2D2 T cells in the presence or absence of $MOG_{35–55}$. (*B*) Analysis of IFN-γ production in cocultures of 2D2 T cells with mixed glia or with BMDM 24 h after MOG peptide treatment. Mixed glia cultures, $n = 4$ biological replicates per genotype; BMDM, $n = 3$ biological replicates per genotype. (*C*) Inhibition of IL-1β/IL-1R signaling with antagonist IL-1RA (0.5 μg/mL) abolished exacerbated cytokine production by *C8KO*^{LysM} cocultures treated with antigen for 48 h. WT, $n = 6$; *C8KO*^{LysM}, $n = 5$. *$P < 0.05$; **$P < 0.0.1$; ***$P < 0.001$; ****$P < 0.0001$.

number of Iba1$^+$ BMDM cells were not significantly different between genotypes and treatment conditions, suggesting that *Casp8* ablation did not cause macrophage death (*SI Appendix*, Fig. S12*B*). This result is consistent with flow cytometry data in which increased IL-1β production by *Casp8*-deficient macrophages was independent of cell death, as Annexin V$^+$, PI$^+$, and Annexin V$^+$/PI$^+$ populations were all comparable between genotypes under both control and LPS-treated conditions (*SI Appendix*, Fig. S10). Taken together, our data suggest that caspase-8 acts as a negative immune-regulator in macrophages licensed by MOG-reactive CD4$^+$ T cells and that loss of caspase-8 in macrophages exacerbate T cell activation.

We next investigated the mechanism by which *Casp8*-deficient BMDM potentiates immune responses of MOG-specific CD4$^+$ T helper cells. Similar to their capability to constitutively process pro–IL-1β when primed with LPS, *Casp8*-deficient BMDM generated significantly higher levels of mature IL-1β than WT BMDM when engaged with CD4$^+$ T cells in the presence of MOG antigen (Fig. 5*C*). Previously, it has been shown that T cell signaling through IL-1 receptor type 1 (IL-1R) is critical for pathogenic cytokine production in EAE progression and that mice lacking *Il1*, *Il1r*, or downstream *Myd88* have compromised EAE development and less disease severity (38, 39). We therefore asked whether elevated BMDM-derived IL-1β due to *Casp8* deficiency engages T cell IL-1R signaling axis to further strengthen pathogenic CD4$^+$ T cell responses. Indeed, IL-1RA, an IL-1R receptor antagonist, nearly completely abolished MOG-dependent IFN-γ, GM-CSF, IL-17A, and IL-23 production by T cells, while it had no effect on the level of IL-1β produced by BMDM (Fig. 5*C*). GM-CSF produced by Th cells is a key contributing signal for CCR2$^+$Ly6C^{hi} monocyte infiltration and encephalitogenicity (3, 40). Our finding is consistent with previous reports demonstrating inflammasome-derived IL-1β acting through the IL-1R/MyD88 signaling axis in T cells to promote GM-CSF production (39). Moreover, intercellular interactions between BMDM and 2D2 T cells are prerequisite for these effects, as in the absence of T cells, neither *Casp8*-deficient nor WT BMDM produced any detectable levels of IL-1β or IFN-γ when treated with $MOG_{35–55}$.

It should be noted that naïve 2D2 T cells were polarized under the Th1 polarization conditions before cocultured with BMDM, since we observed primarily Th1 responses in CNS antigen recall experiments (Fig. 3*F*). The Th1 polarized culture

condition produced ~80% IFN-γ$^+$ Th1 cells, 10% IL-17A$^+$ Th17 cells, and less than 3% IL-4$^+$ Th2 cells as determined by flow cytometry analysis. The data showed that antigen-induced pathogenic cytokines, characteristic of activated Th1 and Th17 cells, were all significantly elevated in cocultures of T cells plus *Casp8*-deficient BMDM and suppressed by blockade of IL-1β/IL-1R signaling (Fig. 5*C*). Other antigen-induced cytokines/chemokines, such as IL-10 and CCL2, were not affected by *Casp8* deficiency or IL-1R antagonism (Fig. 5*C*). Moreover, IL-18, an IL-1 family cytokine processed by inflammasomes, was not significantly impacted by *Casp8* deficiency, suggesting differential caspase-8 regulation of inflammasomes in IL-1β and IL-18 maturation. Collectively, these data suggest that loss of *Casp8* in macrophages potentiates encephalitogenic T cell activation through engaging the IL-1β/IL-1 receptor signaling axis that feed-forward T lymphocyte effector immune responses.

RIPK3 Acts Downstream of Caspase-8 for IL-1β Production in BMDM. Our data revealed that posttranslational processing of pro–IL-1β underlies exacerbated IL-1β produciton by *Casp8*-deficient macrophages in comparison to WT macrophages upon innate immune activation (e.g., LPS) or MOG-reactive T cell engagement. While interactions between caspase-8 and RIPK1/RIPK3 is well recognized, it remains unclear whether RIPK3 mediates NLRP3 inflammasome activation independent of its role in necroptosis. To investigate whether caspase-8 suppression of NLRP3 inflammasome-derived IL-1β in primed macrophages is mediated by RIPK3, we utilized necrostatin-1 (Nec1), a specific RIPK1 kinase inhibitor that prevents RIPK3 phosphorylation (41, 42). Inhibiting RIPK3 activation with Nec1 or *Ripk3* gene deletion both completely abrogated the enhanced IL-1β production in *Casp8*-deficient BMDM (Fig. 6 *A* and *B*), indicating that RIPK3 is positioned at the interface between caspase-8 and inflammasomal processing of IL-1β.

To investigate the role of myeloid RIPK3 in encephalitogenic T cell activation, we next examined the effect of Nec1 and myeloid *Ripk3* ablation in cocultures with T cells. The heightened production of IL-1β, IFN-γ, IL-17A, and GM-CSF due to *Casp8* deficiency were all abolished by Nec1 or loss of *Ripk3* (Fig. 6 *C* and *D*), reinforcing the concept that caspase-8 intrinsically restricts RIPK1/RIPK3 activation. To test whether RIPK3-mediated inflammasome activation is responsible for worsened clinical outcome in *C8KO^{LysM}* mice, we induced EAE in WT, *C8KO^{LysM}*, *C8KO^{LysM}/Ripk3$^{-/-}$*, and *Ripk3$^{-/-}$* mice. Indeed, the exacerbated EAE clinical symptoms observed in *C8KO^{LysM}* mice were normalized in *C8KO^{LysM}/Ripk3* double-knockout mice, which were indistinguishable from WT controls (Fig. 6*E*). In addition, *Ripk3$^{-/-}$* mice displayed a similar disease onset as WT mice but moderately milder disease progression, a finding consistent with previous studies where inhibition of the RIPK1/RIPK3 axis reduces EAE severity (42). Taken together, our findings demonstrated that unrestrained RIPK3-mediated IL-1β production in *Casp8*-deficient macrophages exacerbates inflammatory activation CD4$^+$ Th cells, perpetuating EAE progression during the early phase of the disease.

Discussion

The proinflammatory cytokine IL-1β is a critical mediator in immune defense as well as tissue injury. In this study, we report that caspase-8 constitutively restricts inflammatory macrophages by suppressing NLRP3 inflammasome-mediated IL-1β production when activated by the TLR4 ligand LPS or effector T cells. We found that partially processed caspase-8 is accumulated in macrophage/microglia in MS lesions. Ablation of *Casp8* selectively in myeloid cells, but not CNS resident microglia, resulted in exacerbated neuroinflammation and worse clinical symptoms in the EAE mouse model of MS, which was linked with increased MHCII$^+$ macrophages and CD4$^+$ T cells in the CNS and elevated production of IL-1β and IFN-γ. We further demonstrate that the increased capability of *Casp8*-deficient macrophages to produce IL-1β in comparison to WT cells was dependent on ROS and caspase-1 activity. When instructed by autoreactive CD4$^+$ T helper cells, *Casp8*-deficient macrophages facilitated production of Th1/17 cytokines, such as IFN-γ, IL-17A, and GM-CSF via the paracrine IL-1β/IL-1R signaling axis in an antigen-dependent manner. Importantly, this myeloid *Casp8* deficiency-dependent enhancement of T cell effector immune responses was prevented by RIPK1 inhibition or loss of RIPK3. Moreover, deleting *Ripk3* in *C8KO^{LysM}* mice reversed the worsening effect brought by myeloid *Casp8* ablation in the effector phase of EAE. Together, these data demonstrate that caspase-8 activation in infiltrated macrophages functionally restrains RIPK3-mediated IL-1β maturation, thereby dampening IL-1R–dependent Th1/17 effector function during autoimmune demyelination (*SI Appendix*, Fig. S13).

Under physiological conditions, caspase-8 resides as a procaspase-8 (p55/54) in the cytoplasm and its full activation requires proximity-triggered self-processing into a homodimer of p18/p10 subunits that lead to apoptosis (12). Unprocessed caspase-8 or the intermediate p43/41 caspase-8, which contains the tandem DED-DED domain (tDED) at the N terminal followed by p18, forms a heterodimer with cFLIP$_L$ that controls RIPK1-RIPK3 ripoptosome activation (14, 42). Moreover, caspase-8 can act as a scaffolding protein in inflammatory signaling (12, 15, 43). In the present study, we found the p43/41 form of caspase-8 was consistently elevated in MS brains compared with controls, while the fully active p18 fragment was more variable and overall remains comparable to controls (Fig. 1). Previous studies observed defective caspase-8 activation based on decreased p18 in MS brain lysates (42) but also increased active caspase-8 in cortical microglia in MS tissues when assessed by inhibitor-based labeling (44). We observed marked accumulation of the partially processed p43/41 caspase-8 in MS brain lysates compared to controls, and that the same antibody detecting cleaved caspase-8 fragments (p43/41 and p18) predominantly labled active macrophages/microglia near the lesion. The fact that these macrophage/microglia harbored cleaved caspase-8 without exhibiting any morphological degeneration suggests that the p43/41 caspase-8, not the fully activated caspase-8, may function in regulating inflammation in MS. Consistent with the data from the human MS tissues, caspase-8 is up-regulated in the spinal cord of EAE mice and immunohistochemical analysis shows similar expression patterns of cleaved caspase-8 in Iba1$^+$ cells in demyelinating lesions.

Caspase-8 mediates noncanonical inflammasome activation upon fungal challenges and is also able to directly process pro–IL-1β independent of the inflammasome (34). Due to the embryonic lethality of *Casp8$^{-/-}$* mice, many studies have employed *Casp8$^{-/-}$* immune cells on the *Ripk3$^{-/-}$* background. Using genetic approaches, we found that *Casp8* deficiency in myeloid cells does not abrogate inflammation, but instead results in exacerbated inflammation due to enhanced generation of IL-1β, when challenged by TLR agonist or

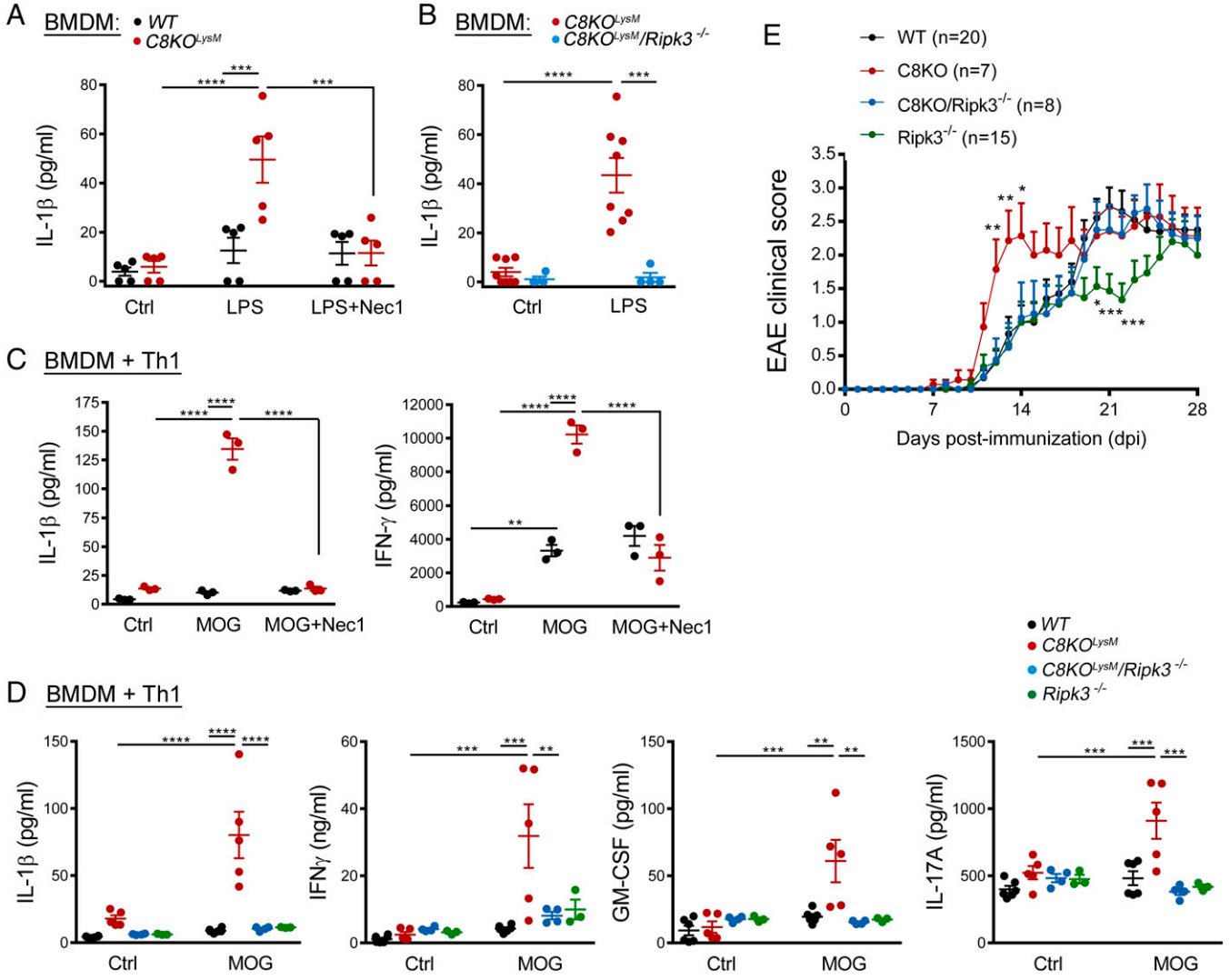

Fig. 6. RIPK3 mediates the heightened IL-1β production, autoimmune responses, and EAE progression evoked by the loss of myeloid caspase-8. (*A* and *B*) Suppression of IL-1β production by RIPK1 inhibition. WT and *C8KO*^{LysM} BMDM were activated with LPS (10 ng/mL) with or without Nec1 (20 μM) for 24 h, and the level of IL-1β was measured in the supernatants. $n = 5$ per genotype. (*B*) *Ripk3* deletion in *C8KO*^{LysM} BMDM completely abrogated LPS-induced production of mature IL-1β. IL-1β was measured in the supernatants at 24 h. *C8KO*^{LysM}, $n = 8$; *C8KO*^{LysM}/*Ripk3*$^{-/-}$, $n = 4$. (*C*) Nec1 inhibited MOG-induced IL-1β and IFN-γ production in *C8KO*^{LysM} BMDM/2D2 T cell cocultures. BMDM were cocultured with Th1 polarized 2D2 T cells in the absence and presence of $MOG_{35–55}$ and Nec1 (20 μM) for 24 h, and cytokines were measured in the supernatants. $n = 3$ per genotype. (*D*) *Ripk3* deletion in *C8KO*^{LysM} BMDM abolished MOG-elicited IL-1β production and resultant production of GM-CSF, IFN-γ, and IL-17A by T cells. *C8KO*^{LysM}, $n = 5$; *C8KO*^{LysM}/*Ripk3*$^{-/-}$, $n = 4$; *Ripk3*$^{-/-}$, $n = 3$. (*E*) Mean clinical scores of mice subjected to MOG-induced EAE. *C8KO*^{LysM}, $n = 7$; *C8KO*^{LysM}/*Ripk3*$^{-/-}$, $n = 8$; WT, $n = 20$; *Ripk3*$^{-/-}$, $n = 15$. Two-way ANOVA with Bonferroni's post hoc multiple test was used to assess statistical significance between groups. *$P < 0.05$; **$P < 0.01$; ***$P < 0.001$; ****$P < 0.0001$. The significance is indicated between *C8KO*^{LysM} and *C8KO*^{LysM}/*Ripk3*$^{-/-}$ and between WT controls and *Ripk3*$^{-/-}$ mice.

licensed by autoreactive T cells. Surprisingly, we found that cleaved caspase-8, most likely in the p43/41 intermediate form, interacts with NLRP3 in the spinal cord lesions of EAE mice, and that *Casp8* deficiency leads to larger NLRP3-containing complexes and more inflammatory MHCII^{+} macrophages and CD4^{+} T cells. Our findings are also in line with those from another report (16) showing that CD11c-driven conditional *Casp8* ablation results in exacerbated RIPK3-mediated NLRP3 inflammasome assembly in LPS endotoxin shock models and in cultured dendritic cells independent of cell death.

Inflammasome plays a central role in innate immunity by detecting and responding to a large range of pathogen-associated and damage-associated molecular patterns (30, 45). Dysregulation of inflammasome-mediated IL-1β has been implicated in MS/EAE pathogeneses (46). Our study suggests that caspase-8 in monocyte-derived macrophages functions as a negative regulator of NLRP3 inflammasome. Direct association of caspase-8 with NLRP3 or ASC has been implicated in cultures based on coimmunoprecipitation and ectopic overexpression analysis (16, 47). Although we did not examine whether other proteins, such as $cFLIP_{L/S}$ or RIPK1/RIPK3, are localized together with caspase-8/NLRP3 oligomers, $cFLIP_L$ is in fact up-regulated in the EAE spinal cord and correlates with decreased caspase-8 p18 (42), likely preventing full caspase-8 activation. Our finding of cleaved caspase-8 colocalized with NLRP3 raises the possibility of direct regulation of NLRP3 inflammasome by caspase-8 signaling platforms in autoimmune inflammatory diseases. Interestingly, caspase-8 containing the tDEDs is able to interact with ASC at inflammasome through heterotypic tDED/PYD interactions (48, 49). As both NLRP3 and ASC are PYD-containing proteins, it would be interesting to examine whether the intermediate p43/41 (tDED-p18) caspase-8 directly interacts with NLRP3 and antagonizes classic NLRP3 inflammasome activation, and whether aberrant accumulation of the intermediate caspase-8 in macrophage/

microglia in MS lesions represents dysregulation or, alternatively, a compensatory mechanism attempting to restrain inflammation. In this regard, a recent study detected increased coexpression of NLRP3 and IL-1β in myeloid cells in active lesions in patients with primary progressive MS (50, 51). Interestingly, *CASP8* polymorphism has been implicated in primary progressive MS (22) and is one of the strongly suggestive autosomal non-MHC loci in MS susceptibility (23). Together, these observations call for further investigation into the potential contribution of caspase-8/NLRP3 inflammasome dysregulation to the pathogenesis of progressive MS.

In an experimental model of autoimmune demyelination, we found that caspase-8 deficiency in myeloid cells results in enhanced neuroinflammation. Using chimeric mice with microglial *Casp8* deletion on a *Ripk3*-null background, a recent study suggested that caspase-8 activated by TLR-mediated IRAMK promotes noncanonical inflammasome formation and inflammation in EAE (44). IRAKM is a negative regulator of the TLR signaling pathway (52) and *Irakm* deficiency exacerbates EAE progression (53). We did not observe significant effects after microglial *Casp8* ablation in our study, nor did we observe differences between WT and caspase-8–deficient microglia in their capacity to engage MOG-specific T cell responses in vitro. However, this does not necessarily exclude immune regulatory functions of microglial caspase-8 under certain neuroinflammatory or neurodegenerative contexts. We observed that *Ripk3*-null mice displayed moderate improvements in EAE clinical scores during the effector phase, which appears to be independent macrophage-driven IL-1β production, in agreement with milder disease progression upon pharmacological inhibition of RIPK1 kinase or loss of RIPK3 (42, 54).

Ripk3 deficiency rescued embryonic lethality of *Casp8*-null mice, underscoring the importance of caspase-8 in restricting RIPK3-mediated pathways in vascular, hematopoietic, and innate immune systems (13). Selective caspase-8 deficiency in myeloid cells, as shown here, rendered macrophages responding more robustly to autoreactive $CD4^+$ T helper cells and TLR activation, leading to IL-1β production via an RIPK3-dependent mechanism that is independent of cell death. Other cytokines, such as TNF-α and IL-6, were not affected. This complete dependence on RIPK3 for IL-1β production also raises a cautionary note on the interpretation of some caspase-8 functions if they are solely based on *Ripk3*-null background, as simultaneous loss of both caspase-8 and RIPK3 may obscure caspase-8 functioning along the RIPK1/RIPK3 axis.

In summary, our data show that caspase-8 blocks RIPK3-mediated IL-1β production independent of cell death in macrophages instructed by encephalitogenic $CD4^+$ T cells, and that IL-1β in turn acts through the IL-1R signaling axis to amplify T cell-driven autoimmune inflammation. This study thus uncovers a mechanistic link between autoimmunity and inflammatory IL-1β production by macrophages that is negatively regulated by caspase-8, and suggests that dysregulation of the caspase-8/RIPK1/RIPK3/IL-1β pathway could contribute to autoimmune inflammatory diseases.

Materials and Methods

Materials. Unless specified otherwise, all reagents were from Sigma-Aldrich. Postmortem brain tissues from patients with clinically diagnosed and pathologically confirmed MS and controls were obtained from the Rocky Mountain MS Center Tissue Bank (Englewood, CO) and the Human Brain and Spinal Fluid Resource Center (Los Angeles, CA), as previously described (55).

Mice and Tamoxifen Treatment. C57BL/6; Cre reporter B6.Cg-Gt(ROSA)26-Sor$^{tm4(CAG-tdTomato)Hze}$ (*R26-tdTomato*, Ai14, Stock No. 007914); B6.129P2-Lyz2$^{tm1(cre)Ifo/J}$ (*LysM-cre,* Stock No. 004781); B6.129P2(Cg)-*Cx3cr1* < tm2.1(cre/ERT)Litt>/WganJ (*Cx3cr1-creER*, Stock No.021160); MOG_{35-55} TCR-transgenic 2D2 mice (Stock No. 006912) were purchased from The Jackson Laboratory. *Ripk3*-deficient mice were a generous gift from Xiaodong Wang, National Institute of Biological Sciences, Beijing, China (56). *Casp8* floxed transgenic (*Casp8*$^{fl/fl}$) mice were a gift from Stephen Hedrick, University of California, San Diego (57). In the *loxP*-flanked *Casp8* allele, exon 3 was deleted upon cre-mediated recombination. *Casp8* conditional mice, *LysM*$^{cre/+}$*Casp8* $^{fl/fl}$ and *Cx3cr1*$^{creERt/+}$*Casp8*$^{fl/fl}$, were generated by breeding *Casp8*$^{fl/fl}$ with *LysM*$^{cre/+}$ and *Cx3cr1*$^{creERt/+}$, respectively. Both male and female mice were used in the study. All mice were housed under constant 12-h light/dark cycles in covered cages and fed with standard rodent diet ad libitum under specific pathogen-free conditions at the Comparative Medicine Program, Texas A&M University. Tamoxifen-induced cre recombination in adult mice was carried out as described previously (29). Briefly, 4- to 5-wk-old littermate control *Casp8*$^{fl/fl}$ (WT) and *C8KO*^{Cx3cr1ERt} mice were treated twice with 8 mg tamoxifen in 200 μL corn oil via oral gavage at 48-h apart. All experiments were reviewed and approved by the Institutional Animal Care and Use Committee of the Texas A&M University.

EAE Induction. EAE was induced as previously described with modifications (29, 32). Eight- to 12-wk-old, both female and male WT, *C8KO*^{lysM}, or *C8KO*^{Cx3cr1} mice were immunized subcutaneously with 200 μg MOG_{35-55} (MEVGWYRSPFSRVVHLYRNGK; AS-60130-10, AnaSpec) emulsified in complete Freund's adjuvant (263910, Difco) containing 200 μg/mL or 500 μg/mL of heat-killed *M. tuberculosis* (H37 Ra, 231141, Difco). Mice were injected with 400 ng pertussis toxin intraperitoneally on days 0 and 2. From day 7 postimmunization, mice were weighed daily, and EAE clinical scores were determined based on a 5 scoring scale (58): 0.5, tail weakness; 1, tail paresis; 1.5, reversible impaired righting reflex; 2, impaired righting reflex, limp tail, and weakness of hindlimb; 2.5, limp tail and unable to support trunk due to extreme rear limb paresis; 3, paralysis of one hindlimb; 4, paralysis of both hindlimbs; 4.5, paralysis of both hindlimbs and forelimb paresis; 5, moribund or death. Mashed food and easier access to freshwater were supplied when the animals reached an EAE clinical score of 2.

2D2 T Cell Isolation and Coculture with BMDM. $CD4^+$ T cells were isolated from the spleen of 8- to 12-wk-old naive 2D2 mice using BD-iMAG kit (BD Bioscience) as described previously (29). In brief, 2×10^7 of mononuclear cells were resuspended in 3% FBS/PBS at a density of 2×10^7/mL and incubated with biotinylated anti-CD4 antibody (13-0042, eBioscience) for 15 min on ice. After being washed twice with iMAG buffer (552361, BD Bioscience), the cells were resuspended at a density of 4×10^7 cells/mL and incubated with BD iMAG streptavidin particle (10 μL per 1.0×10^7 cells) at 8 °C for 30 min. The labeled cells were separated by placing the tube in a cell separation magnet (552311, BD Biosciences) for 10 min. Unbound leukocytes (negative portion) were washed out by removing the solution while the tube was still attached to the magnet. This step was repeated for a total of three times to increase selection purity. Positively selected $CD4^+$ cells were then resuspended in a complete RPMI medium. $CD4^+$ cells (4×10^6) were polarized toward Th1 with α-CD3 (2.5 μg/mL; #16-0031-85, eBioscience), IL-12 (10 ng/mL; #14-8121-62, eBioscience), and α-IL-4 (10 μg/mL; #16-7041-85, eBioscience) in the presence of irradiated feeder cells (2×10^7) for 3 d followed by 4 d of resting in complete RPMI medium containing 10% FBS. Irradiated feeder cells were prepared by irradiating the acutely isolated splenocytes at 3,000 rad (30 Gy). At the end of Th1 polarization, live T cells were purified using Ficoll gradient. $CD4^+$ T cells (1.5×10^4) were then cocultured with BMDM (1.5×10^4) in 96-wells in the complete RPMI medium and treated with or without 25 μg/mL MOG_{35-55} for 2 d.

Flow Cytometry. Single-cell suspensions were preincubated with constant immunoglobulin Fragment (Fc)-receptor blocking antibody (anti-CD16/CD32, Clone 93, #14-0161, eBioscience) to block nonspecific binding. The cells were incubated with fluorophore-conjugated antibodies specific for ms CD4 APC (#17-0041), ms CD8 FITC (#11-0081), ms CD11b FITC (#11-0112c), ms CD45 APC (#17-0451-82), ms CD19 PE (#12-0193), ms B220 PE cy5.5 (#45-042-80), ms Ly6G PE (#61-9668, clone 1A8), and ms MHC II PE (#12-5321-81) for 30 min at room temperature followed by washing twice with 500 μL PBS-2% FBS. Flow cytometry data were acquired with Accuri C6 (BD Biosciences) equipped with 488-nm and 633-nm lasers. Color compensation was applied uniformly to all

samples using negative-stained and single-stained control. Data analysis was performed using FlowJo software.

Intracellular ROS Analysis. Intracellular ROS production was evaluated by flow cytometry using H_2DCF-DA (ALX-610-022, Enzo Life Sciences). Briefly, BMDM at the end of treatments were incubated with 25 μM H_2DCF-DA for 30 min at 37 °C. After washing with warm HBSS, the cells were resuspended in 100 μL of PBS containing 2% FBS and analyzed immediately using a flow cytometer equipped with a 488-nm laser for excitation (Accuri C6, BD Biosciences).

Statistical Analysis. GraphPad Prism software was used for data analyses. Unless otherwise indicated, data were expressed as mean ± SEM. When appropriate, differences between two groups were analyzed with a two-tailed Student's *t* test. Differences between more than two groups were analyzed with multivariate ANOVA followed by Bonferroni's post hoc test. All of the datasets were tested for normal distribution using the D'Agostino-Pearson omnibus normality test to confirm the normal distribution. For the dataset that did not pass the normality test, a nonparametric method using Mann–Whitney *U* test was applied to define the significance as indicated in the figure legends. Differences were considered to be statistically significant when $P < 0.05$.

Data Availability. All study data are included in the main text and *SI Appendix*.

ACKNOWLEDGMENTS. We thank Dr. Xiaodong Wang for providing Ripk3 mice; Dr. Beiyan Zhou for assistance with flow cytometry; Dr. Andrew Hillhouse for technical support with multiplex immunoassay; Dr. Roula Mouneimne for helping with confocal microscopy; J.L. laboratory members for technical assistance and discussions; and Dr. Jane Welsh for comments on the manuscript. Human tissue specimens were kindly provided by the Rocky Mountain MS Center (supported by the National Multiple Sclerosis Society) and the Human Brain and Spinal Fluid Resource Center of the VA West Los Angeles Healthcare Center (sponsored by National Institute of Neurological Disorders and Stroke/National Institute of Mental Health, National Multiple Sclerosis Society, and Department of Veterans Affairs). Some illustrations were created with BioRender (https://biorender.com). This study was funded in part by grants from the NIH (R01NS060017, R21NS093487) and the National Multiple Sclerosis Society (RG1507, RG1703).

1. C. Lucchinetti *et al.*, Heterogeneity of multiple sclerosis lesions: Implications for the pathogenesis of demyelination. *Ann. Neurol.* **47**, 707–717 (2000).
2. B. Ajami, J. L. Bennett, C. Krieger, K. M. McNagny, F. M. V. Rossi, Infiltrating monocytes trigger EAE progression, but do not contribute to the resident microglia pool. *Nat. Neurosci.* **14**, 1142–1149 (2011).
3. A. L. Croxford *et al.*, The cytokine GM-CSF drives the inflammatory signature of CCR2+ monocytes and licenses autoimmunity. *Immunity* **43**, 502–514 (2015).
4. B. Tummers, D. R. Green, Caspase-8: Regulating life and death. *Immunol. Rev.* **277**, 76–89 (2017).
5. D. Wallach, T.-B. Kang, Programmed cell death in immune defense: Knowledge and presumptions. *Immunity* **49**, 19–32 (2018).
6. R. Feltham, J. E. Vince, K. E. Lawlor, Caspase-8: Not so silently deadly. *Clin. Transl. Immunology* **6**, e124 (2017).
7. S. J. Kim, J. Li, Caspase blockade induces RIP3-mediated programmed necrosis in Toll-like receptor-activated microglia. *Cell Death Dis.* **4**, e716 (2013).
8. J. Yuan, P. Amin, D. Ofengeim, Necroptosis and RIPK1-mediated neuroinflammation in CNS diseases. *Nat. Rev. Neurosci.* **20**, 19–33 (2019).
9. S. Kang *et al.*, Caspase-8 scaffolding function and MLKL regulate NLRP3 inflammasome activation downstream of TLR3. *Nat. Commun.* **6**, 7515 (2015).
10. T. P. Monie, C. E. Bryant, Caspase-8 functions as a key mediator of inflammation and pro-IL-1β processing via both canonical and non-canonical pathways. *Immunol. Rev.* **265**, 181–193 (2015).
11. B. Tummers *et al.*, Caspase-8-dependent inflammatory responses are controlled by its adaptor, FADD, and necroptosis. *Immunity* **52**, 994–1006.e8 (2020).
12. C. M. Henry, S. J. Martin, Caspase-8 acts in a non-enzymatic role as a scaffold for assembly of a pro-inflammatory "FADDosome" complex upon TRAIL stimulation. *Mol. Cell* **65**, 715–729.e5 (2017).
13. W. J. Kaiser *et al.*, RIP3 mediates the embryonic lethality of caspase-8-deficient mice. *Nature* **471**, 368–372 (2011).
14. A. Oberst *et al.*, Catalytic activity of the caspase-8-FLIP(L) complex inhibits RIPK3-dependent necrosis. *Nature* **471**, 363–367 (2011).
15. N. H. Philip *et al.*, Activity of uncleaved caspase-8 controls anti-bacterial immune defense and TLR-induced cytokine production independent of cell death. *PLoS Pathog.* **12**, e1005910 (2016).
16. T. B. Kang, S. H. Yang, B. Toth, A. Kovalenko, D. Wallach, Caspase-8 blocks kinase RIPK3-mediated activation of the NLRP3 inflammasome. *Immunity* **38**, 27–40 (2013).
17. A. Kovalenko *et al.*, Caspase-8 deficiency in epidermal keratinocytes triggers an inflammatory skin disease. *J. Exp. Med.* **206**, 2161–2177 (2009).
18. A. Rajput *et al.*, RIG-I RNA helicase activation of IRF3 transcription factor is negatively regulated by caspase-8-mediated cleavage of the RIP1 protein. *Immunity* **34**, 340–351 (2011).
19. J. Rehker *et al.*, Caspase-8, association with Alzheimer's disease and functional analysis of rare variants. *PLoS One* **12**, e0185777 (2017).
20. A. C. Gomes *et al.*, Decreased levels of CD95 and caspase-8 mRNA in multiple sclerosis patients with gadolinium-enhancing lesions on MRI. *Neurosci. Lett.* **352**, 101–104 (2003).
21. A. Achiron, M. Gurevich, N. Friedman, N. Kaminski, M. Mandel, Blood transcriptional signatures of multiple sclerosis: Unique gene expression of disease activity. *Ann. Neurol.* **55**, 410–417 (2004).
22. M. Camiña-Tato *et al.*, Genetic association of CASP8 polymorphisms with primary progressive multiple sclerosis. *J. Neuroimmunol.* **222**, 70–75 (2010).
23. International Multiple Sclerosis Genetics Consortium, Multiple sclerosis genomic map implicates peripheral immune cells and microglia in susceptibility. *Science* **365**, eaav7188 (2019).
24. M. B. Johnson *et al.*, Single-cell analysis reveals transcriptional heterogeneity of neural progenitors in human cortex. *Nat. Neurosci.* **18**, 637–646 (2015).
25. Y. Zhang *et al.*, An RNA-sequencing transcriptome and splicing database of glia, neurons, and vascular cells of the cerebral cortex. *J. Neurosci.* **34**, 11929–11947 (2014).
26. Y. Lavin *et al.*, Tissue-resident macrophage enhancer landscapes are shaped by the local microenvironment. *Cell* **159**, 1312–1326 (2014).
27. L. Bö *et al.*, Detection of MHC class II-antigens on macrophages and microglia, but not on astrocytes and endothelia in active multiple sclerosis lesions. *J. Neuroimmunol.* **51**, 135–146 (1994).
28. S. H. Wong, L. Santambrogio, J. L. Strominger, Caspases and nitric oxide broadly regulate dendritic cell maturation and surface expression of class II MHC proteins. *Proc. Natl. Acad. Sci. U.S.A.* **101**, 17783–17788 (2004).
29. H. C. Lu *et al.*, STAT3 signaling in myeloid cells promotes pathogenic myelin-specific T cell differentiation and autoimmune demyelination. *Proc. Natl. Acad. Sci. U.S.A.* **117**, 5430–5441 (2020).
30. D. Gris *et al.*, NLRP3 plays a critical role in the development of experimental autoimmune encephalomyelitis by mediating Th1 and Th17 responses. *J. Immunol.* **185**, 974–981 (2010).
31. M. Inoue, K. L. Williams, M. D. Gunn, M. L. Shinohara, NLRP3 inflammasome induces chemotactic immune cell migration to the CNS in experimental autoimmune encephalomyelitis. *Proc. Natl. Acad. Sci. U.S.A.* **109**, 10480–10485 (2012).
32. M. Inoue *et al.*, Interferon-β therapy against EAE is effective only when development of the disease depends on the NLRP3 inflammasome. *Sci. Signal.* **5**, ra38 (2012).
33. C. Antonopoulos *et al.*, Caspase-8 as an effector and regulator of NLRP3 inflammasome signaling. *J. Biol. Chem.* **290**, 20167–20184 (2015).
34. P. Gurung *et al.*, FADD and caspase-8 mediate priming and activation of the canonical and noncanonical Nlrp3 inflammasomes. *J. Immunol.* **192**, 1835–1846 (2014).
35. J. E. Vince *et al.*, Inhibitor of apoptosis proteins limit RIP3 kinase-dependent interleukin-1 activation. *Immunity* **36**, 215–227 (2012).
36. K. Schroder, J. Tschopp, The inflammasomes. *Cell* **140**, 821–832 (2010).
37. M. E. Heid *et al.*, Mitochondrial reactive oxygen species induces NLRP3-dependent lysosomal damage and inflammasome activation. *J. Immunol.* **191**, 5230–5238 (2013).
38. S. J. Lalor *et al.*, Caspase-1-processed cytokines IL-1beta and IL-18 promote IL-17 production by gammadelta and CD4 T cells that mediate autoimmunity. *J. Immunol.* **186**, 5738–5748 (2011).
39. J. R. Lukens, M. J. Barr, D. D. Chaplin, H. Chi, T. D. Kanneganti, Inflammasome-derived IL-1β regulates the production of GM-CSF by CD4(+) T cells and γδ T cells. *J. Immunol.* **188**, 3107–3115 (2012).
40. M. El-Behi *et al.*, The encephalitogenicity of T(H)17 cells is dependent on IL-1- and IL-23-induced production of the cytokine GM-CSF. *Nat. Immunol.* **12**, 568–575 (2011).
41. A. Degterev *et al.*, Identification of RIP1 kinase as a specific cellular target of necrostatins. *Nat. Chem. Biol.* **4**, 313–321 (2008).
42. D. Ofengeim *et al.*, Activation of necroptosis in multiple sclerosis. *Cell Rep.* **10**, 1836–1849 (2015).
43. T. B. Kang, S. H. Yang, B. Toth, A. Kovalenko, D. Wallach, Activation of the NLRP3 inflammasome by proteins that signal for necroptosis. *Methods Enzymol.* **545**, 67–81 (2014).
44. C. J. Zhang *et al.*, TLR-stimulated IRAKM activates caspase-8 inflammasome in microglia and promotes neuroinflammation. *J. Clin. Invest.* **128**, 5399–5412 (2018).
45. T. Matsuki, S. Nakae, K. Sudo, R. Horai, Y. Iwakura, Abnormal T cell activation caused by the imbalance of the IL-1/IL-1R antagonist system is responsible for the development of experimental autoimmune encephalomyelitis. *Int. Immunol.* **18**, 399–407 (2006).
46. V. Govindarajan, J. P. de Rivero Vaccari, R. W. Keane, Role of inflammasomes in multiple sclerosis and their potential as therapeutic targets. *J. Neuroinflammation* **17**, 260 (2020).
47. K. Newton *et al.*, Activity of caspase-8 determines plasticity between cell death pathways. *Nature* **575**, 679–682 (2019).
48. P. R. Vajjhala *et al.*, The inflammasome adaptor ASC induces procaspase-8 death effector domain filaments. *J. Biol. Chem.* **290**, 29217–29230 (2015).
49. T. M. Fu *et al.*, Cryo-EM structure of caspase-8 tandem DED filament reveals assembly and regulation mechanisms of the death-inducing signaling complex. *Mol. Cell* **64**, 236–250 (2016).
50. S. Malhotra *et al.*, NLRP3 inflammasome as prognostic factor and therapeutic target in primary progressive multiple sclerosis patients. *Brain* **143**, 1414–1430 (2020).
51. A. Kadowaki, F. J. Quintana, The NLRP3 inflammasome in progressive multiple sclerosis. *Brain* **143**, 1286–1288 (2020).
52. K. Kobayashi *et al.*, IRAK-M is a negative regulator of Toll-like receptor signaling. *Cell* **110**, 191–202 (2002).
53. B. Liu *et al.*, Interleukin-1 receptor associated kinase (IRAK)-M -mediated type 2 microglia polarization ameliorates the severity of experimental autoimmune encephalomyelitis (EAE). *J. Autoimmun.* **102**, 77–88 (2019).
54. S. Zhang *et al.*, RIP1 kinase inhibitor halts the progression of an immune-induced demyelination disease at the stage of monocyte elevation. *Proc. Natl. Acad. Sci. U.S.A.* **116**, 5675–5680 (2019).
55. S. Kim, A. J. Steelman, Y. Zhang, H. C. Kinney, J. Li, Aberrant upregulation of astroglial ceramide potentiates oligodendrocyte injury. *Brain Pathol.* **22**, 41–57 (2012).
56. S. He, Y. Liang, F. Shao, X. Wang, Toll-like receptors activate programmed necrosis in macrophages through a receptor-interacting kinase-3-mediated pathway. *Proc. Natl. Acad. Sci. U.S.A.* **108**, 20054–20059 (2011).
57. D. R. Beisner, I. L. Ch'en, R. V. Kolla, A. Hoffmann, S. M. Hedrick, Cutting edge: Innate immunity conferred by B cells is regulated by caspase-8. *J. Immunol.* **175**, 3469–3473 (2005).
58. I. M. Stromnes, J. M. Goverman, Passive induction of experimental allergic encephalomyelitis. *Nat. Protoc.* **1**, 1952–1960 (2006).